On the Ribosomal Density that Maximizes Protein Translation Rate

Yoram Zarai, Michael Margaliot, and Tamir Tuller*

arXiv:1607.04064v1 [q-bio.GN] 14 Jul 2016

Abstract

During mRNA translation, several ribosomes attach to the same mRNA molecule simultaneously translating it into a protein. This pipelining increases the protein production rate. A natural and important question is what ribosomal density maximizes the protein production rate. Using mathematical models of ribosome flow along both a linear and a circular mRNA molecule we prove that typically the steady-state production rate is maximized when the ribosomal density is one half of the maximal possible density. We discuss the implications of our results to endogenous genes under natural cellular conditions and also to synthetic biology.

Index Terms

Systems biology, synthetic biology, mRNA translation, ribosome flow model, protein production rate, maximizing production rate, ribosomal average density.

I. Introduction

The transformation of the genetic information in the DNA into functional proteins is called *gene expression*. Two important steps in gene expression are *transcription* of the DNA code into messenger RNA (mRNA) by RNA polymerase (RNAP), and then *translation* of the mRNA into proteins. During translation, complex macromolecules called ribosomes traverse the mRNA strand, decoding it codon by codon into a corresponding chain of amino-acids that is folded co- and post-translationally to become a functional protein [1]. The rate in which proteins are produced during the translation step is called the protein translation rate or protein production rate.

According to current knowledge, translation takes place in all living organisms and under all conditions. Understanding the numerous factors that affect this dynamical process has important implications to many scientific disciplines including medicine, evolutionary biology, synthetic biology, and more.

Computational models of translation are becoming increasingly important as the amount of experimental findings related to translation rapidly increases (see, e.g. [64], [11], [16], [23], [51], [50], [9], [42], [13], [36]). Such models are particularly important in the context of synthetic biology and biotechnology, as they can provide predictions on the qualitative and quantitative effects of various manipulations of the genetic machinery. Recent advances in measuring translation in *real time* [56], [55], [28], [53] will further increase the interest in computational models that can integrate and explain the measured biological data.

During translation, a large number of ribosomes act simultaneously on the same mRNA molecule. This pipelining of the protein production leads to a more continuous production rate and increased efficiency. Indeed, the production rate may reach 5 [15] new peptide bonds per second in eukaryotes [prokaryotes] (see [57]).

The ribosomal density along the mRNA molecule may affect different fundamental intracellular phenomena. A very high density can lead to ribosomal traffic jams, collisions and abortions. It may also

The research of MM and TT is partially supported by research grants from the Israeli Ministry of Science, Technology, and Space, and the Binational Science Foundation. The research of MM is also supported by a research grant from the Israel Science Foundation

Y. Zarai is with the School of Elec. Eng., Tel-Aviv University, Tel-Aviv 69978, Israel. E-mail: yoramzar@mail.tau.ac.il

M. Margaliot is with the School of Elec. Eng. and the Sagol School of Neuroscience, Tel-Aviv University, Tel-Aviv 69978, Israel. E-mail: michaelm@eng.tau.ac.il

T. Tuller (corresponding author) is with the Dept. of Biomedical Eng. and the Sagol School of Neuroscience, Tel-Aviv University, Tel-Aviv 69978, Israel. E-mail: tamirtul@post.tau.ac.il

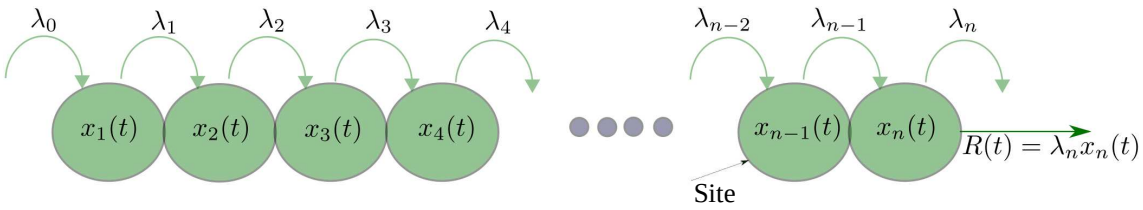

Fig. 1. The RFM models unidirectional flow along a chain of n sites. The state variable $x_i(t) \in [0, 1]$ represents the density of site i at time t. The parameter $\lambda_i > 0$ controls the transition rate from site i to site $i + 1$, with λ_0 [λ_n] controlling the initiation [exit] rate. The output rate at time t is $R(t) = \lambda_n x_n(t)$.

contribute to co-translational misfolding of proteins. On the other hand, a very low ribosomal density may lead to a low production rate, and a high degradation rate of mRNA molecules [14], [18], [19], [15], [63], [52], [34]. Thus, a natural and important question is what ribosomal density optimizes one (or more) intracellular phenomena, for example, the protein production rate. Optimizing the protein production rate is also an important challenge in synthetic biology and biotechnology, where a standard objective is to maximize the translation efficiency and protein levels of heterologous genes in a new host (see, e.g., [21, Chapter 9].

In this paper, we analyze the density that maximizes the translation rate using a mathematical model of ribosome flow along the mRNA molecule. A standard mathematical model for ribosome flow is the *totally asymmetric simple exclusion process* (TASEP) [43], [65]. In this model, particles hop unidirectionally along an ordered lattice of L sites. Every site can be either free or occupied by a particle, and a particle can only hop to a free site. This simple exclusion principle models particles that have "volume" and thus cannot overtake one other. The hops are stochastic, and the rate of hoping from site i to site $i+1$ is denoted by γ_i. A particle can hop to [from] the first [last] site of the lattice at a rate α [β]. The average flow through the lattice converges to a steady-state value that depends on the parameters $L, \alpha, \gamma_1, \ldots, \gamma_{L-1}, \beta$. Analysis of TASEP in non trivial, and closed-form results have been obtained mainly for the homogeneous TASEP (HTASEP), i.e. for the case where all the γ_is are assumed to be equal.

TASEP has become a fundamental model in non-equilibrium statistical mechanics, and has been applied to model numerous natural and artificial processes [41]. In the context of translation, the lattice models the mRNA molecule, the particles are ribosomes, and simple exclusion means that a ribosome cannot overtake a ribosome in front of it.

TASEP has two standard configurations. In TASEP with *open boundary conditions* the two sides of the chain are connected to two particle reservoirs, and particles can hop into the chain (if the first site is empty) and out of the chain (if the last site is full). In TASEP with *periodic boundary conditions* the chain is closed, and a particle that hops from the last site returns to the first one. Thus, here the particles hop around a ring, and the number of particles is conserved.

The *ribosome flow model* (RFM) [40] is a continuous-time, deterministic, compartmental model for the unidirectional flow of "material" along an open chain of n consecutive compartments (or sites). The RFM can be derived via a dynamic mean-field approximation of TASEP with open boundary conditions [41, section 4.9.7] [3, p. R345]. The RFM includes n state-variables, denoted $x_1(t), \ldots x_n(t)$, with $x_i(t)$ describing the amount (or density) of "material" in site i at time t, normalized such that $x_i(t) = 1$ [$x_i(t) = 0$] indicates that site i is completely full [completely empty] at time t. In the RFM, the two sides of the chain are connected to two particle reservoirs. A parameter $\lambda_i > 0$, $i = 0, \ldots, n$, controls the transition rate from site i to site $i + 1$, where λ_0 [λ_n] is the initiation [exit] rate (see Fig. 1).

In the *ribosome flow model on a ring (RFMR)* [38] the particles exiting the last site enter the first site. This is the mean-field approximation of TASEP with periodic boundary conditions. Since the number of particles is conserved, the RFMR admits a first integral. Both the RFM and RFMR are cooperative dynamical systems [44], but their dynamical properties turn out to be quite different [38].

The RFM [RFMR] has been applied to model and analyze ribosome flow along an open [circular] mRNA molecule during translation. Indeed, it is well known that in eukaryotes the mRNA is often (temporarily)

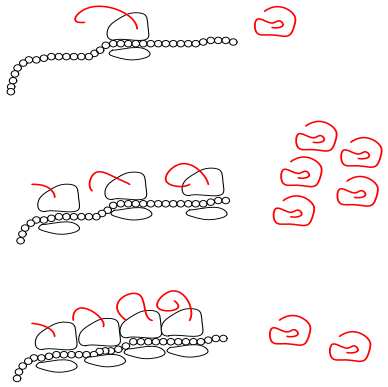

Fig. 2. Ribosome density and production rate. Too few ribosomes (upper figure) lead to a low production rate, as do too many ribosomes (lower figure) due to traffic jams along the mRNA. Optimal production is achieved when the density is one half of the maximal possible density (middle figure).

circularized, for example, by translation initiation factors [54]. In addition, circular RNA forms appear in all domains of life [12], [10], [7], [6], [17], [4], [5].

Here, we use the RFM [RFMR] to analyze the ribosomal density along a linear [circular] mRNA molecule that maximizes the steady-state protein production rate. We refer to this density as the *optimal density*. This problem has already been studied before. For example, Zouridis and Hatzimanikatis [66] derived a deterministic, sequence-specific kinetic model for translation and studied the effect of the average ribosomal density on the steady-state production rate. Their model assumes homogeneous elongation rates and open-boundary conditions, and includes all the elementary steps involved in the elongation cycle at every codon. Their simulations suggest that there exists a unique average density that corresponds to a maximal production rate, see Figures 2A and 5A in [66] (see also [37]).

The RFM and RFMR are simpler models and thus allow to rigorously prove several analytic results on the optimal density. For a circular mRNA, we prove that there always exists a unique optimal density that maximizes the steady-state production rate, and that it can be determined efficiently using a simple "hill climbing" algorithm. In addition, we show that under certain symmetry conditions on the rates the optimal density is one half of the maximal possible density.

In the case of a linear mRNA molecule, we prove that when the initiation and elongations rates are chosen to optimize the production rate, under an affine constraint on the rates, the corresponding optimal density is one half of the maximal possible density (see Fig. 2).

The remainder of this paper is organized as follows. The next section briefly reviews the RFM and the RFMR. Section III describes our main results. The proofs of all the results are placed in the Appendix. The final section summarizes the results, describes their biological implications, and suggests several directions for further research.

II. The Ribosome Flow Model

The dynamics of the RFM with n sites is given by n nonlinear first-order ordinary differential equations:

$$\begin{aligned}
\dot{x}_1 &= \lambda_0(1-x_1) - \lambda_1 x_1(1-x_2),\\
\dot{x}_2 &= \lambda_1 x_1(1-x_2) - \lambda_2 x_2(1-x_3),\\
\dot{x}_3 &= \lambda_2 x_2(1-x_3) - \lambda_3 x_3(1-x_4),\\
&\vdots\\
\dot{x}_{n-1} &= \lambda_{n-2} x_{n-2}(1-x_{n-1}) - \lambda_{n-1} x_{n-1}(1-x_n),\\
\dot{x}_n &= \lambda_{n-1} x_{n-1}(1-x_n) - \lambda_n x_n. \qquad (1)
\end{aligned}$$

If we define $x_0(t) := 1$ and $x_{n+1}(t) := 0$ then (1) can be written more succinctly as

$$\dot{x}_i = \lambda_{i-1}x_{i-1}(1 - x_i) - \lambda_i x_i(1 - x_{i+1}), \quad i = 1, \ldots, n. \tag{2}$$

This equation can be explained as follows. The change in the density in site i is the flow from site $i-1$ to site i minus the flow from site i to site $i+1$. The latter is $\lambda_i x_i(t)(1-x_{i+1}(t))$. This flow is proportional to $x_i(t)$, i.e. it increases with the density at site i, and to $(1-x_{i+1}(t))$, i.e. it decreases as site $i+1$ becomes fuller. In particular, when the site is completely full, i.e. $x_{i+1}(t) = 1$, there is no flow into this site. This corresponds to a "soft" version of a simple exclusion principle: the flow of particles into a site decreases as that site becomes fuller. Note that the maximal possible flow from site i to site $i+1$ is the ith transition rate λ_i. The output rate from the chain is $R(t) := \lambda_n x_n(t)$.

Let $x(t, a)$ denote the solution of (1) at time $t \geq 0$ for the initial condition $x(0) = a$. Since the state-variables correspond to normalized occupation levels, we always assume that a belongs to the closed n-dimensional unit cube: $C^n := \{x \in \mathbb{R}^n : x_i \in [0, 1], i = 1, \ldots, n\}$. It is straightforward to verify that this implies that $x(t, a) \in C^n$ for all $t \geq 0$. In other words, C^n is an invariant set of the dynamics [25].

Let $\mathrm{int}(C^n)$ denote the interior of C^n. It was shown in [25] that the RFM is a *cooperative dynamical system* [44] and that this implies that (1) admits a *unique* steady-state point $e = e(\lambda_0, \ldots, \lambda_n) \in \mathrm{int}(C^n)$ that is globally asymptotically stable, that is, $\lim_{t\to\infty} x(t, a) = e$ for all $a \in C^n$ (see also [24]). In particular, this means that the production rate converges to the steady-state value:

$$R := \lambda_n e_n. \tag{3}$$

For $x = e$ the left-hand side of all the equations in (1) is zero, so

$$\begin{aligned}
\lambda_0(1 - e_1) &= \lambda_1 e_1(1 - e_2) \\
&= \lambda_2 e_2(1 - e_3) \\
&\vdots \\
&= \lambda_{n-1} e_{n-1}(1 - e_n) \\
&= \lambda_n e_n \\
&= R.
\end{aligned} \tag{4}$$

This yields

$$\begin{aligned}
e_n &= R/\lambda_n, \\
e_{n-1} &= R/(\lambda_{n-1}(1 - e_n)), \\
&\vdots \\
e_2 &= R/(\lambda_2(1 - e_3)), \\
e_1 &= R/(\lambda_1(1 - e_2)),
\end{aligned} \tag{5}$$

and

$$e_1 = 1 - R/\lambda_0. \tag{6}$$

Combining (5) and (6) provides an elegant *finite continued fraction* [22] expression for R:

$$0 = 1 - \cfrac{R/\lambda_0}{1 - \cfrac{R/\lambda_1}{1 - \cfrac{R/\lambda_2}{\ddots \; 1 - \cfrac{R/\lambda_{n-1}}{1 - R/\lambda_n.}}}} \tag{7}$$

Note that this equation admits several solutions for R, however, we are interested only in the unique feasible solution, i.e. the solution corresponding to $e \in \mathrm{int}(C^n)$. Note also that (7) implies that

$$R(c\lambda_0, \ldots, c\lambda_n) = cR(\lambda_0, \ldots, \lambda_n), \quad \text{for all } c > 0, \tag{8}$$

that is, $R(\lambda_0, \ldots, \lambda_n)$ is a *homogeneous function* of degree one. Ref. [32] proved that $R(\lambda_0, \ldots, \lambda_n)$ is a *strictly concave* function on $\mathbb{R}^{n+1}_{++}$.

A. Ribosome Flow Model on a Ring

If we consider the RFM with the additional assumption that all the ribosomes leaving site n circulate back to site 1 then we obtain the RFMR:

$$\begin{aligned}
\dot{x}_1 &= \lambda_n x_n(1 - x_1) - \lambda_1 x_1(1 - x_2), \\
\dot{x}_2 &= \lambda_1 x_1(1 - x_2) - \lambda_2 x_2(1 - x_3), \\
&\vdots \\
\dot{x}_n &= \lambda_{n-1} x_{n-1}(1 - x_n) - \lambda_n x_n(1 - x_1).
\end{aligned} \tag{9}$$

This can also be written succinctly as (2), but now with every index interpreted modulo n. In particular, λ_0 [x_0] is replaced by λ_n [x_n].

For $p \in \mathbb{R}$, let p_n denote the column vector $\begin{bmatrix} p & p & \ldots & p \end{bmatrix}^T \in \mathbb{R}^n$. Eq. (9) implies that

$$\frac{d}{dt}(1_n^T x(t)) \equiv 0, \text{ for all } t \geq 0,$$

so the *ribosome density* $H(x) := 1_n^T x$ is conserved, i.e.

$$H(x(t)) = H(x(0)), \quad \text{for all } t \geq 0. \tag{10}$$

The dynamics of the RFMR thus redistributes the particles between the sites, but without changing ribosome density. In the context of translation, this means that the total number of ribosomes on the (circular) mRNA is conserved.

For $s \in [0, n]$, denote the s *level set* of H by

$$L_s := \{y \in C^n : 1_n^T y = s\}.$$

It was shown in [38] that the RFMR is a strongly cooperative dynamical system, that every level set L_s contains a unique equilibrium point $e = e(s, \lambda_1, \ldots, \lambda_n)$, and that any trajectory of the RFMR emanating from any $x(0) \in L_s$ converges to this equilibrium point. For example if $s = 0$, corresponding to the initial condition $x(0) = 0_n$, then $x(t) \equiv 0_n$ for all $t \geq 0$, so $e = 0_n$. Similarly, $s = n$ corresponds to the initial condition $x(0) = 1_n$ and then clearly $x(t) \equiv 1_n$ for all $t \geq 0$, so $e = 1_n$. Since these two cases are trivial, below we will always assume that $s \in (0, n)$. In this case, $e \in \mathrm{int}(C^n)$.

Let $R = R(s, \lambda_1, \ldots, \lambda_n)$ denote the steady-state production rate in the RFMR for $x(0) \in L_s$. It is straightforward to verify that for any $c > 0$

$$R(s, c\lambda_1, \ldots, c\lambda_n) = cR(s, \lambda_1, \ldots, \lambda_n). \tag{11}$$

For more on the analysis of the RFM and the RFMR using tools from systems and control theory, see [61], [32], [33], [38], [26], [60]. For a general discussion on using systems and control theory in systems biology see the excellent survey papers by Sontag [45], [46].

The RFM models translation on a single isolated mRNA molecule. A network of RFMs, interconnected through a common pool of "free" ribosomes has been used to model simultaneous translation of several mRNA molecules while competing for the available ribosomes [39]. It is important to note that many analysis results for the RFM, RFMR, and networks of RFMs hold for any set of transition rates. This is in contrast to the analysis results on the TASEP model. Rigorous analysis of TASEP seems to be tractable only under the assumption that the internal hopping rates are all equal (i.e. the homogeneous case).

The next section describes our main results on the optimal ribosome density.

III. Main Results

Let $\rho(t) := \frac{1}{n}(1_n^T x(t))$ denote the average ribosome density along the mRNA molecule at time t. Recall that for every set of parameters in our models the state-variables converge to a steady-state e. In particular, $\rho(t)$ converges to the steady-state average ribosomal density:

$$\rho := \frac{1}{n}(1_n^T e).$$

Note that since $e_i \in [0,1]$ for all i, $\rho \in [0,1]$. We are interested in analyzing the density that is obtained when the parameter values in the model are the ones that maximize the steady-state production rate.

A. Optimal Density in the RFMR

Recall that in the RFMR the dynamical behavior depends on the rates and the quantity $s := 1_n^T x(0)$. The ribosomal density is constant: $\rho(t) \equiv s/n$. Fix arbitrary transition rates $\lambda_i > 0$, $i = 1, \ldots, n$, and let $R(s) := R(s; \lambda_1, \ldots, \lambda_n)$ and $e(s) := e(s; \lambda_1, \ldots, \lambda_n)$ denote the steady-state production rate and the ribosomal densities, respectively, as a function of s. The next result shows that there always exists a unique density $\rho^* = s^*/n$ that corresponds to a maximal steady-state production rate.

Proposition 1 *For any set of rates $\lambda_i > 0$ in the RFMR there exists a unique value $s^* = s^*(\lambda_1, \ldots, \lambda_n) \in (0, n)$ that maximizes $R(s)$. Furthermore, for this optimal value $e^* := e(s^*)$ and $R^* := R(s^*)$ satisfy*

$$e_1^* \ldots e_n^* = (1 - e_1^*) \ldots (1 - e_n^*), \tag{12}$$

and

$$(R^*)^n = (\lambda_1 \ldots \lambda_n)(e_1^* \ldots e_n^*)^2. \tag{13}$$

The proof of this result (given in the Appendix) shows that $R(s)$ is strictly increasing on $[0, s^*)$ and strictly decreasing on $(s^*, n]$, so a simple "hill climbing" algorithm can be used to find s^*.

The optimality condition (12) can be explained as follows. If s is very small then there will not be enough ribosomes on the circular mRNA and the production rate will be small (for example, for $s = 0$ we have $e = 0_n$, and thus $R = \lambda_1 e_1(1 - e_2) = 0$). In this case, the product of the e_is is small, so $e_1 \ldots e_n < (1 - e_1) \ldots (1 - e_n)$ and (12) does not hold. If s is very large traffic jams evolve on the mRNA and again the production rate will be small (for example, for $s = n$ we have $e = 1_n$, and thus $R = \lambda_1 e_1(1 - e_2) = 0$). In this case, $e_1 \ldots e_n > (1 - e_1) \ldots (1 - e_n)$ and (12) does not hold. Thus, (12) describes the point where the balance between too few and too many ribosomes is optimal.

The next example demonstrates Proposition 1 in a special case.

Example 1 Consider an RFMR with $\lambda_1 = \cdots = \lambda_n$, i.e. all the rates are equal. Denote their common value by λ_c. Then it follows from (9) that $1_n c$, $c > 0$, is an equilibrium point. By uniqueness of the equilibrium point in every level set of H this implies that $e = (s/n)1_n$, and thus $R = \lambda_n e_n(1 - e_1) = \lambda_c(s/n)(1 - (s/n))$. Thus, $\frac{\partial R}{\partial s} = \frac{\lambda_c}{n^2}(n - 2s)$, so $R(s)$ is strictly increasing [decreasing] on $s \in [0, n/2]$

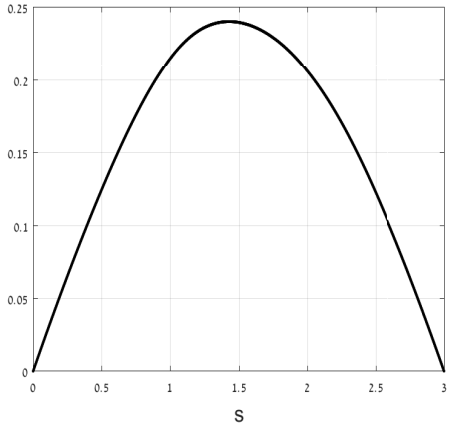

Fig. 3. Steady-state production rate $R(s)$ as a function of s for the RFMR in Example 2.

$[s \in [n/2, n]]$ and therefore attains a unique maximum at $s^* = n/2$. Then $e^* := e(s^*) = (1/2)1_n$ and $R^* := R(s^*) = \lambda_c/4$, and it is straightforward to verify that (12) and (13) hold. Note also that $\frac{\partial^2 R}{\partial s^2} = -\frac{2\lambda_c}{n^2} < 0$, implying that $R(s)$ is a strictly concave function. □

The next example demonstrates the dependence of $R(s)$ on s when the rates are not homogeneous.

Example 2 Consider an RFMR with dimension $n = 3$ and transition rates $\lambda_1 = 2$, $\lambda_2 = 6$, and $\lambda_3 = 1/3$. Fig. 3 depicts $R(s)$ for $s \in [0, 3]$. It may be seen that $R(s)$ attains a unique maximum at $s^* = 1.4268$ (all numerical values in this paper are to four digit accuracy). The corresponding equilibrium point is $e^* = \begin{bmatrix}0.1862 & 0.3539 & 0.8867\end{bmatrix}^T$, and the optimal production rate is $R^* = \lambda_1 e_1^*(1-e_2^*) = 0.2405$. Fig. 4 depicts a histogram of the equilibrium point e for three values of the level set parameter: $s = 1/2$, $s = 1.4268$, and $s = 2$. Note that e_3 is the maximal entry in e for all s. This is due to fact that the entry rate $\lambda_2 = 6$ into site 3 is high, and the exit rate $\lambda_3 = 1/3$ from site 3 is low. □

In order to better understand Fig. 4 note that the equilibrium point in the RFMR satisfies

$$e_1 + \cdots + e_n = s,$$

and, by (9),

$$\begin{aligned}\lambda_n e_n(1 - e_1) &= \lambda_1 e_1(1 - e_2),\\ &= \lambda_2 e_2(1 - e_3),\\ &\vdots\\ &= \lambda_{n-1} e_{n-1}(1 - e_n).\end{aligned} \tag{14}$$

Let $k_i := \lambda_1 \dots \lambda_{i-1}\lambda_{i+1} \dots \lambda_n$, $i = 1, \dots, n$, and let $\mu := \sum_{i=1}^n k_i$. If $s \approx 0$ then all the e_is will be small, so we can ignore the terms $1 - e_i$ in (14), and this yields $e_i \approx \frac{k_i s}{\mu}$, $i = 1, \dots, n$. A similar argument shows that if $s \approx n$ then $e_i \approx 1 - \frac{k_{i-1}(n-s)}{\mu}$, $i = 1, \dots, n$. For the particular case in Example 2 this implies that when $s \approx 0$ $e \approx (s/22)\begin{bmatrix}3 & 1 & 18\end{bmatrix}^T$. In particular, $e_2 < e_1 < e_3$. When $s \approx 3$, $e \approx (s/22)\begin{bmatrix}18s - 32 & 3s + 13 & s + 19\end{bmatrix}^T$. In particular, $e_1 < e_2 < e_3$.

For small values of n it is possible to give more explicit results.

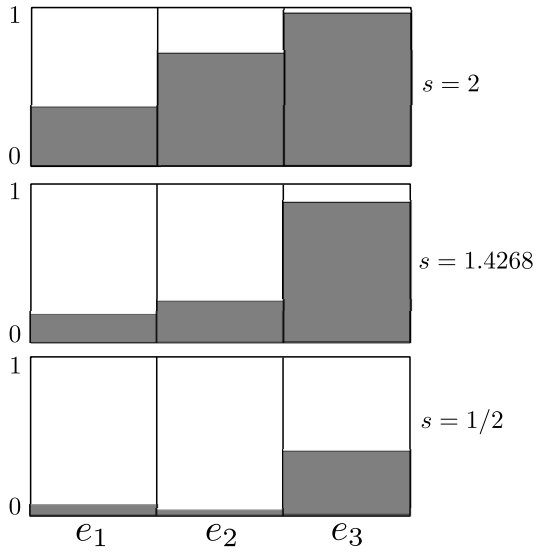

Fig. 4. Equilibrium point e in Example 2 for three different s values.

Fact 1 *For an RFMR with $n = 2$ the optimal values are $s^* = 1$ and*

$$R^* = \frac{\lambda_1\lambda_2}{(\sqrt{\lambda_1} + \sqrt{\lambda_2})^2}. \tag{15}$$

For an RFMR with $n = 3$ the optimal production rate satisfies:

$$2\sqrt{\lambda_1\lambda_2\lambda_3}(R^*)^{3/2} + (\lambda_1\lambda_2 + \lambda_1\lambda_3 + \lambda_2\lambda_3)R^* - \lambda_1\lambda_2\lambda_3 = 0. \tag{16}$$

Let $e_i' := \frac{\partial}{\partial s}e_i$ denote the sensitivity of e_i with respect to a change in the total density s. The next results provides an expression for these sensitivities at the equilibrium point corresponding to the optimal density.

Proposition 2 *Consider an RFMR with dimension n. Fix rates $\lambda_i > 0$, and let $s^* = s^*(\lambda_1, \ldots, \lambda_n)$ and $e^* = e^*(\lambda_1, \ldots, \lambda_n)$ be as defined in Proposition 1. Then $(e^*)' = \frac{v}{1_n^T v}$, where*

$$v := \begin{bmatrix} \frac{e_1^* \ldots e_{n-1}^*}{(1-e_2^*)\ldots(1-e_n^*)} & \frac{e_2^* \ldots e_{n-1}^*}{(1-e_3^*)\ldots(1-e_n^*)} & \ldots & \frac{e_{n-1}^*}{1-e_n^*} & 1 \end{bmatrix}^T. \tag{17}$$

Example 3 Consider again the RFMR in Example 2. Recall that here $s^* = 1.4268$ and $e^* = \begin{bmatrix}0.1862 & 0.3539 & 0.8867\end{bmatrix}$. Substituting this in (17) yields $v = \begin{bmatrix}0.9002 & 3.1236 & 1\end{bmatrix}^T$, so $(e^*)' = \begin{bmatrix}0.1792 & 0.6218 & 0.1991\end{bmatrix}^T$. This means that if we change the density from s^* to $\bar{s} := s^* + \varepsilon$ then the steady-state production rate changes from R^* to

$$\begin{aligned} \bar{R} &= \lambda_1\bar{e}_1(1 - \bar{e}_2) \\ &= \lambda_1(e_1^* + \varepsilon(e_1^*)')(1 - e_2^* - \varepsilon(e_2^*)') + O(\varepsilon^2) \\ &= R^* + \lambda_1\varepsilon((1 - e_2^*)(e_1^*)' - e_1^*(e_2^*)') + O(\varepsilon^2), \end{aligned}$$

and substituting the numerical values yields

$$\bar{R} = R^* + O(\varepsilon^2).$$

Indeed, this agrees with the fact that the graph of $R(s)$ attains a maximum at s^*. □

In Example 2 above the optimal value s^* is close, but not equal to $n/2 = 3/2$. The next result provides a symmetry condition guaranteeing that $s^* = n/2$, that is, that the optimal density is equal to one half of

the maximal possible density.

Proposition 3 *If the transition rates in the RFMR satisfy*

$$\lambda_i = \lambda_{n-i}, \quad i = 1, \ldots, n, \tag{18}$$

then $s^* = n/2$ *and* $e_i^* = e_{n+1-i}^*$ *for all* i*.*

Thus, in this case the optimal mean density is $\rho^* = (n/2)/n = 1/2$. Note that condition (18) always holds for $n = 2$. Also, since a cyclic permutation of the rates leads to an RFMR with the same behavior, it is enough that (18) holds for some cyclic permutation of the rates. For $n = 3$ this holds if at least two of the rates $\lambda_1, \lambda_2, \lambda_3$ are equal.

We note that a result similar to Proposition 3 is known for the *homogeneous* TASEP with periodic boundary conditions, i.e. that a loading of 50% maximizes the steady-state flow (see, for example, the fundamental diagram in [41, Figure 4.1]).

B. Optimal Density in the RFM

Due to the open boundary conditions in the RFM, the number of particles along the chain is not conserved. Thus, in this section we analyze the steady-state densities corresponding to the rates that yield a maximal steady-state production rate. To do this, we recall the optimization problem posed in [32].

Problem 1 *Fix parameters* $b, w_0, w_1, \ldots, w_n > 0$*. Maximize* $R = R(\lambda_0, \ldots, \lambda_n)$*, with respect to its parameters* $\lambda_0, \ldots, \lambda_n$*, subject to the constraints:*

$$\begin{aligned} \sum_{i=0}^{n} w_i \lambda_i &\leq b, \\ \lambda_0, \ldots, \lambda_n &\geq 0. \end{aligned} \tag{19}$$

In other words, maximize the steady-state production rate given an affine constraint on the rates. Here b is the "total biocellular budget", and the positive values w_i, $i = 0, \ldots, n$, can be used to provide a different weighting to the different rates.

This formulation is motivated by the fact that the biological resources are of course limited. For example, all tRNA molecules are transcripted by the same transcription factors (TFIIIB) and by RNA polymerase III. Hence, if the production of a specific tRNA is increased then the production of some other tRNA must decrease. The total cost b captures this, as any increase in one of the λ_is must be compensated by a decrease in some other rate.

Problem 1 formalizes, using the RFM, an important problem in both systems biology and biotechnology, namely, determine the transition rates that maximize the protein production rate, given the limited biomolecular budget.

It has been shown in [32] that the optimal solution $\lambda_0^*, \ldots, \lambda_n^*$ always satisfies $\sum_{i=0}^{n} w_i \lambda_i^* = b$. Of course, by scaling the w_is we may always assume that $b = 1$. Combining this with the strict concavity of the steady-state production rate $R(\lambda_0, \ldots, \lambda_n)$ in the RFM implies that Problem 1 is a *convex optimization problem* that admits a unique optimal solution $\lambda^* \in \mathbb{R}_{++}^{n+1}$. This solution can thus be found efficiently using numerical algorithms that scale well with n. Here, our goal is to determine what is the steady-state density when the optimal rates are used, that is, when the rates are the solution of Problem 1. We refer to this as the optimal density. Let e_i^*, $i = 1, \ldots, n$, denote the steady-state density at site i corresponding to the optimal rates $\lambda_0^*, \ldots, \lambda_n^*$.

Example 4 Using a simple numerical algorithm we solved 10^5 instances of Problem 1 for an RFM with length $n = 11$ and total budget $b = 1$. In each instance the weights w_i were drawn independently from a uniform distribution over the interval $[0, 1]$. For each instance, we computed the optimal rates λ_i^*s and the

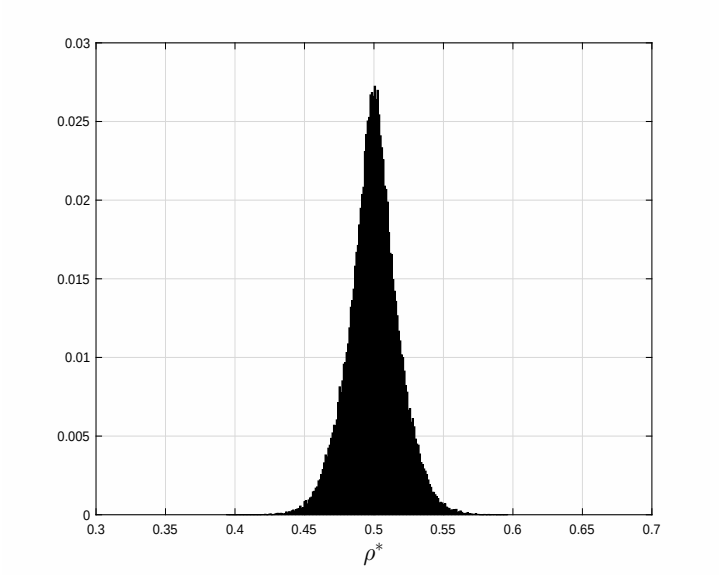

Fig. 5. Normalized histogram of the value ρ^* in Example 4.

corresponding mean steady-state optimal density $\rho^* := \frac{1}{n}\sum_{i=1}^n e_i^*$. Fig. 5 depicts a normalized histogram (that is, the empirical probability) of the 10^5 values of ρ^*. It may be observed that typically ρ^* is close to $1/2$. Similar results are obtained when the weights are drawn using other statistics, e.g. exponential, Rayleigh, and Gamma distributions. □

In the case where all the weights are equal we can also derive theoretical results on the structure of e^* and thus of ρ^*.

1) Homogeneous Affine Constraint: Consider the case where all the weights w_i in Problem 1 are equal. We refer to this as the *homogeneous constraint* case. Indeed, in this case the weights give equal preference to all the rates, so if the corresponding optimal solution satisfies $\lambda_i^* > \lambda_j^*$ for some i, j then this implies that, in the context of maximizing R, λ_i is "more important" than λ_j. By (8), we may assume in this case, without loss of generality, that $w_0 = \cdots = w_n = b = 1$, so the constraint is

$$\sum_{i=0}^{n} \lambda_i \leq 1. \tag{20}$$

Proposition 4 *Consider Problem 1 with the homogeneous constraint* (20)*. Then the optimal steady-state occupancies satisfy*

$$e_i^* = 1 - e_{n-i+1}^*, \quad i = 1, \ldots, n. \tag{21}$$

If n is even then

$$e_1^* > \cdots > e_{\frac{n}{2}}^* > \frac{1}{2} > e_{\frac{n}{2}+1}^* > \cdots > e_n^*, \tag{22}$$

and if n is odd then

$$e_1^* > \cdots > e_{\frac{n-1}{2}}^* > e_{\frac{n+1}{2}}^* = \frac{1}{2} > e_{\frac{n+2}{2}}^* > \cdots > e_n^*. \tag{23}$$

In both cases, the corresponding optimal density is $\rho^* = 1/2$.

Proposition 4 implies that under the homogeneous constraint the steady-state occupancies corresponding to the optimal solution decrease along the chain, and are anti-symmetric with respect to the center of the chain, i.e. $e_i^* - 1/2 = 1/2 - e_{n-i+1}^*$, $i = 1, \ldots, n$. This immediately implies that $\rho^* = \frac{1}{n}\sum_{i=1}^n e_i^* = 1/2$.

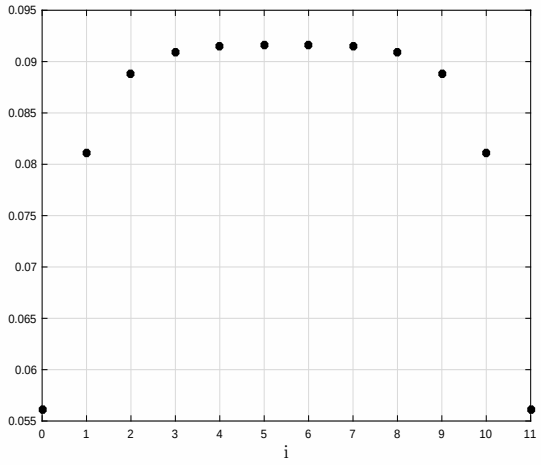

Fig. 6. Optimal rates λ_i^* as a function of i for an RFM with $n = 11$ and the homogeneous constraint (20).

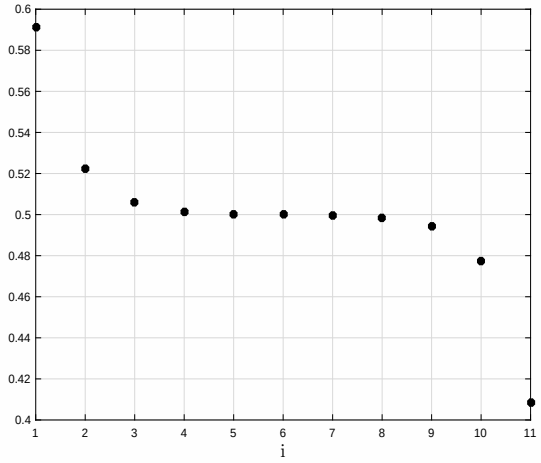

Fig. 7. Optimal steady-state ribosome distribution e_i^* as a function of i for an RFM with $n = 11$ and the homogeneous constraint (20).

Example 5 Consider Problem 1 for an RFM with $n = 11$ and the homogeneous constraint (20). Fig. 6 depicts the optimal values λ_i^*, $i = 0, \ldots, 11$. It may be seen that the λ_i^*s are symmetric, i.e. $\lambda_i^* = \lambda_{11-i}^*$, and that they increase towards the center of the chain. The corresponding steady-state distribution is $e^* = [0.5913, 0.5224, 0.5059, 0.5016, 0.5004, 0.5000, 0.4996, 0.4984, 0.4941, 0.4776, 0.4087]^T$ (see Fig. 7). It may be seen that the steady-state densities strictly decrease along the chain and are anti-symmetric with respect to the center of the chain. □

Since the RFM [RFMR] is the dynamic mean-field approximation of TASEP with open [periodic] boundary conditions, our results naturally lead to questions on the optimal density in TASEP. These questions seem to be difficult to analyze rigorously. We used a simple grid search to address the problem of maximizing the steady-state flow in HTASEP (with all internal rates equal to one) with respect to the parameters α and β subject to the constraint $w_1\alpha + w_2\beta = b$. For $L = 11$ and $w_1 = w_2 = b = 1$ the solution is $\alpha^* = \beta^* = 1/2$, and the corresponding steady-state occupancies (computed using [3, Eq. (3.65)]) are all equal to $1/2$. Thus the average optimal density is $\rho^* = 1/2$.

We also ran 10000 tests with w_1 and w_2 chosen from an independent uniform distribution on $[0, 1]$. In each case, a simple grid-search was used to find the optimal rates. Fig. 8 depicts a normalized histogram of the optimal steady-state sum of ribosome densities in an HTASEP with $L = 30$. It may be seen that the typical optimal density is about $1/2$. A similar result has been reported in [27] that used TASSEP with a superposition of open and periodic boundary conditions.

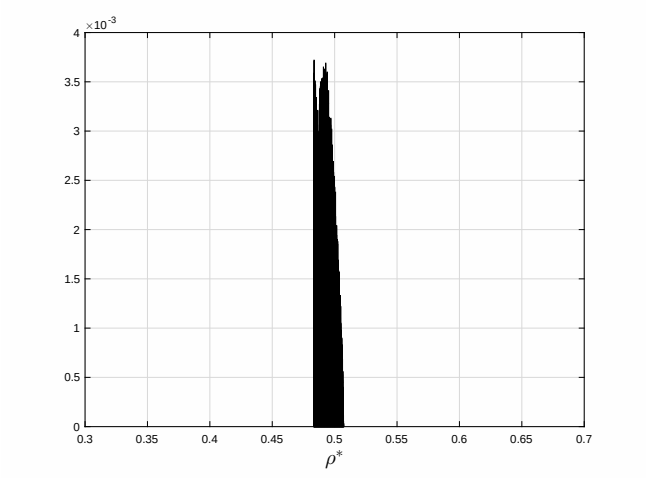

Fig. 8. Normalized histogram of steady-state mean optimal ribosome density in HTASEP with $N = 30$ and optimal parameters.

These simulation results corroborate the analytic results derived above for the RFM and RFMR.

IV. Discussion

A natural analogy for the cell is that of a factory operating complex and inter-dependent biosynthesis assembly processes [35]. Increasing the production rate can be done by both operating several identical processes in parallel, and by pipelining every single process. In the context of translation, many mRNA copies of the same gene are translated in parallel, and the same transcript is simultaneously translated by several ribosomes. A natural question is what is the density of ribosomes along the transcript that leads to a *maximal* production rate. It is clear that a very small density will not be optimal, and since the ribosomes interact and may jam each other, a very high density is also not optimal.

We studied this question using dynamical models for ribosome flow in both a linear and a circular mRNA molecule. Our results show that typically the optimal density is close to one half of the maximal density.

In synthetic biology and biotechnology optimizing the translation rate is a standard goal, and we believe that our results can provide guidelines for designing and reengineering transcripts. However, in vivo biological regulation of mRNA translation may have several goals besides optimizing the production rate. For endogenous genes there are many additional constraints that shape the transcript, translation rates, and ribosome densities. For example, it is known that evolution optimizes not only protein levels, but also attempts to minimize their production cost [49], [20]. This cost may include for example the biocellular budget required for producing the ribosomes themselves. Thus, we do not expect that the protein levels of all genes will be maximal. Rather, we expect that translation is optimized for proteins that are required with high copy numbers (e.g. those related to house keeping genes and some structural genes).

Furthermore, it is important to mention that there are various additional constraints shaping the coding regions of endogenous genes. These include various regulatory signals related to various gene expression steps, co-translational folding, and the functionality of the protein [52], [58], [63], [29], [8], [47]. Thus, under these additional constraints we do not necessarily expect to see ribosome densities that maximize the translation rate.

Indeed, experimental studies of ribosome densities in various organisms demonstrate that on average $15\% - 20\%$ of the mRNA is occupied by ribosomes [2], [31]. However, in 241 genes in *S. cerevisiae* more than 40% of the mRNA is occupied by ribosomes [2]. This suggests that a ribosome density that is close to 0.5 is frequent in certain *specific* mRNA molecules. In addition, it seems that under stress conditions ribosomal densities (and traffic jams) increase (see, e.g. [48]). Thus, under such conditions we expect more mRNAs with ribosome densities close to 0.5 (see, for example, [30]).

Interestingly, the reported results are also in agreement with genome-wide simulations of the RFM that were performed based on the modeling of all the endogenous genes of *S. cerevisiae*, as reported in [40]. Indeed, Fig. 4C there shows the ribosome density, averaged over all the sites of all the mRNAs, as a function of the initiation rate. The maximal production rate corresponds to an average density of about 0.5.

We note in passing that for an RFM with dimension n, with all the rates equal (i.e. $\lambda_0 = \cdots = \lambda_n$), the average ribosomal density is $1/2$ for all n, and that for an RFM with dimension n, $\lambda_0 \to \infty$, and equal elongation rates (i.e. $\lambda_1 = \cdots = \lambda_n$), the average ribosomal density is $\frac{n+1}{2n}$, thus approaching $1/2$ as n increases [62].

Further studies may consider optimizing the translation rate under various additional constraints. For example, it will be interesting to study the optimal ribosome density when taking into account also the biocellular cost of protein production, or under given constraints on the allowed density profile, etc. In addition, it will be interesting to study the optimal densities in more comprehensive models that include competition for the free ribosomes between several mRNA molecules [39]. Another important issue, that is not captured by the RFM and RFMR, is that every ribosome covers several codons. Developing and analyzing RFM/RFMR models with "extended objects" is an important challenge.

Finally, TASEP has been used to model and analyze many other natural and artificial processes including traffic flow and the movement of motor proteins. The problem of the optimal density is of importance in these applications as well.

ACKNOWLEDGMENTS

We thank Gilad Poker for helpful comments.

APPENDIX: PROOFS

Proof of Proposition 1. It follows from known results on the solutions of ODEs that e_i is continuous in s for all i. It is known that every e_i is strictly increasing in s [38, Theorem 1]. Hence, there exists a set E of measure zero such that for all i and all $s \in [0,n] \setminus E$ the derivative $e_i' := \frac{d}{ds} e_i$ exists, and is strictly positive. The steady-state production rate satisfies $R = \lambda_i e_i (1 - e_{i+1})$, for all $i = 1, \ldots, n$. This yields

$$R' = \lambda_i (e_i'(1 - e_{i+1}) - e_i e_{i+1}'), \tag{24}$$

for all i and all $s \in [0,n] \setminus E$.

Let $\mathrm{sgn}(\cdot) : \mathbb{R} \to \{-1, 0, 1\}$ denote the sign function, i.e.

$$\mathrm{sgn}(y) = \begin{cases} 1, & y > 0, \\ 0, & y = 0, \\ -1, & y < 0. \end{cases}$$

We require the following result.

Proposition 5 *For any $s \in [0,n] \setminus E$,*

$$\mathrm{sgn}(R') = \mathrm{sgn}(\prod_{i=1}^{n}(1 - e_i) - \prod_{i=1}^{n} e_i).$$

Proof of Proposition 5. Assume that $R' > 0$. Then (24) yields

$$e_i'(1 - e_{i+1}) > e_i e_{i+1}', \quad i = 1, \ldots, n.$$

Multiplying these n inequalities, and using the fact that $e_i' > 0$ for all i yields

$$\prod_{i=1}^{n}(1 - e_i) > \prod_{i=1}^{n} e_i. \tag{25}$$

To prove the converse implication, assume that (25) holds. Multiplying both sides of the inequality by the strictly positive term $\prod_{j=1}^{n} e'_i$ yields

$$\prod_{i=1}^{n} a_i > \prod_{i=1}^{n} b_i,$$

where $a_i := e'_i(1-e_{i+1})$, and $b_i := e_i e'_{i+1}$. This means that $a_\ell > b_\ell$ for some index $\ell \in \{1,\dots,n\}$. Since $R' = \lambda_\ell(a_\ell - b_\ell)$, it follows that $R' > 0$. Thus, we showed that $R' > 0$ if and only if $\prod_{i=1}^{n}(1-e_i) > \prod_{i=1}^{n} e_i$. The proof that $R' < 0$ if and only if $\prod_{i=1}^{n}(1-e_i) < \prod_{i=1}^{n} e_i$ is similar. This implies that $R' = 0$ if and only if $\prod_{i=1}^{n}(1-e_i) = \prod_{i=1}^{n} e_i$, and this completes the proof of Proposition 5. ■

We can now complete the proof of Proposition 1. Let $p(s) := \prod_{i=1}^{n}(1-e_i)$, and $q(s) := \prod_{i=1}^{n} e_i$. Then $p(0) = 1$, $p(n) = 0$, $q(0) = 0$, and $q(n) = 1$. The strict monotonicity of every e_i implies that $p(s)$ [$q(s)$] is a strictly decreasing [increasing] function in the interval $s \in [0,n]$. This implies that there is a unique $s^* \in [0,n]$ such that $p(s^*) = q(s^*)$. By Proposition 5, this is the unique maximizer of $R(s)$, and for $s = s^*$:

$$e_1^* \dots e_n^* = (1-e_1^*)\dots(1-e_n^*). \tag{26}$$

Also,

$$\begin{aligned} R^* &= \lambda_1 e_1^*(1-e_2^*) \\ &= \lambda_2 e_2^*(1-e_3^*) \\ &\vdots \\ &= \lambda_n e_n^*(1-e_1^*), \end{aligned} \tag{27}$$

and this yields $(R^*)^n = (\lambda_1 \dots \lambda_n)(e_1^* \dots e_n^*)((1-e_1^*)\dots(1-e_n^*))$. Using (26) completes the proof of Proposition 1. ■

Proof of Fact 1. For $n = 2$, (26) yields $e_1^* + e_2^* = 1$, and substituting this in (27) yields (15). Consider the case $n = 3$. Let $\lambda := \lambda_1\lambda_2\lambda_3$. It follows from (27) that

$$\begin{aligned} \lambda_2\lambda_3 R^* &= \lambda e_1^*(1-e_2^*), \\ \lambda_1\lambda_3 R^* &= \lambda e_2^*(1-e_3^*), \\ \lambda_1\lambda_2 R^* &= \lambda e_3^*(1-e_1^*). \end{aligned}$$

Summing these equations yields

$$\eta R^* = \lambda s^* - \lambda(e_1^* e_2^* + e_2^* e_3^* + e_3^* e_1^*), \tag{28}$$

where $\eta := \lambda_2\lambda_3 + \lambda_1\lambda_3 + \lambda_1\lambda_2$. It follows from (26) that

$$e_1^* e_2^* + e_2^* e_3^* + e_3^* e_1^* = s^* - 1 + 2e_1^* e_2^* e_3^*,$$

and substituting this in (28) yields $\eta R^* = \lambda(1 - 2e_1^* e_2^* e_3^*)$. Applying (13) completes the proof. ■

Proof of Proposition 2. Write (24) as

$$D(e^*)' = C(e^*)', \tag{29}$$

where $D := \mathrm{diag}(1-e_2^*, 1-e_3^*, \dots, 1-e_n^*, 1-e_1^*)$, and

$$C := \begin{bmatrix} 0 & e_1^* & 0 & 0 & \dots & 0 & 0 \\ 0 & 0 & e_2^* & 0 & \dots & 0 & 0 \\ & & \vdots & & & & \\ 0 & 0 & 0 & 0 & \dots & 0 & e_{n-1}^* \\ e_n^* & 0 & 0 & 0 & \dots & 0 & 0 \end{bmatrix}.$$

Note that C is cyclic of order n, so multiplying (29) by C^{n-1} yields

$$H(e^*)' = (e_1^* \dots e_n^*)(e^*)', \tag{30}$$

where $H := C^{n-1}D$. In other words, $(e^*)'$ is an eigenvector of H corresponding to the eigenvalue $(e_1^* \dots e_n^*)$. The cyclic structure of C implies that

$$C^{n-1} = \begin{bmatrix} 0 & 0 & \dots & 0 & \mu_1^* \\ \mu_2^* & 0 & \dots & 0 & 0 \\ & & \vdots & & \\ 0 & \dots & \mu_{n-1}^* & 0 & 0 \\ 0 & 0 & \dots & \mu_n^* & 0 \end{bmatrix},$$

where $\mu_i^* := e_i^* e_{i+1}^* \dots e_{i+n-2}^*$, with all indexes interpreted modulo n (e.g., $e_{n+1}^* = e_1^*$). Now it is straightforward to verify that $(e^*)' = cv$, with $c \neq 0$, is the only solution of (30). Since every e_i increases with s, we conclude that $c > 0$. Furthermore, $\sum_{i=1}^n e_i^* = s$ implies that $\sum_{i=1}^n (e_i^*)' = 1$, and this completes the proof. ■

Proof of Proposition 3. The proof follows immediately from the following result.

Proposition 6 *Consider an RFMR with dimension n, and suppose that the transition rates satisfy $\lambda_i = \lambda_{n-i}$ for all i. Then*

1) *$e_i^* = e_{n+1-i}^*$ for any i;*
2) *$R(s) = R(n-s)$ for any $s \in [0, n]$, and $R(s_1) < R(s_2)$ for any $0 \leq s_1 < s_2 \leq n/2$.*

This means in particular that $R(s)$ is symmetric with respect to $s = n/2$, and is strictly increasing in the interval $[0, n/2)$.

Proof of Proposition 6. Given an RFMR with dimension n, and rates λ_i, $i = 1, \dots, n$, let $\bar{x}_i(t) := 1 - x_{n+1-i}(t)$, $i = 1, \dots, n$. Then using the equation

$$\dot{x}_i = \lambda_{i-1} x_{i-1}(1 - x_i) - \lambda_i x_i (1 - x_{i+1})$$

yields

$$\dot{\bar{x}}_i = \bar{\lambda}_{i-1} \bar{x}_{i-1}(1 - \bar{x}_i) - \bar{\lambda}_i \bar{x}_i (1 - \bar{x}_{i+1}),$$

with $\bar{\lambda}_i := \lambda_{n-i}$ (recall that all indexes are interpreted modulo n). This is again an RFMR. Fix an arbitrary $s \in [0, n]$. Then for any $x(0)$ such that $1_n^T x(0) = s$ we have $1_n^T \bar{x}(0) = n - s$. Therefore, the x system converges to $e = e(s, \lambda_1, \dots, \lambda_n)$, and the $\bar{x}$ system to $\bar{e} = e(n - s, \bar{\lambda}_1, \dots, \bar{\lambda}_n)$. This implies that $e_i(s, \lambda_1, \dots, \lambda_n) = 1 - e_{n+1-i}(n - s, \bar{\lambda}_1, \dots, \bar{\lambda}_n)$ for all i. The steady-state production rate in the $\bar{x}$ system is

$$\begin{aligned} \bar{R} &= \bar{\lambda}_n \bar{e}_n (1 - \bar{e}_1) \\ &= \lambda_n (1 - e_1) e_n \\ &= R. \end{aligned}$$

If the rates satisfy $\lambda_i = \lambda_{n-i}$ for all i then $e_i(s) = 1 - e_{n+1-i}(s)$ for all i, and $R(s) = R(n-s)$. By Proposition 1, this means that $R^* = R(n/2)$. Combining this with the results in the proof of Proposition 1 completes the proof of Proposition 6. ■

Proof of Proposition 4. Consider Problem 1 and the homogeneous constraint (20). By [59, Proposition 4]:

$$e_i^* = 1 - e_{n-i+1}^*, \tag{31}$$

and

$$\frac{\lambda_i^*}{\lambda_{i-1}^*} = \frac{e_i^*}{1 - e_i^*}, \tag{32}$$

$i = 1, \ldots, n$, and by [59, Theorem 1]:

$$\lambda_0^* < \lambda_1^* < \cdots < \lambda_{\lfloor n/2 \rfloor}^*, \tag{33}$$

and

$$\lambda_i^* = \lambda_{n-i}^*, \quad i = 0, \ldots, n. \tag{34}$$

Thus, (31) proves (21), and combining (33), (34), and (32) yield (22) and (23). ■

REFERENCES

[1] B. Alberts, A. Johnson, J. Lewis, M. Raff, K. Roberts, and P. Walter, *Molecular Biology of the Cell*. New York: Garland Science, 2008.

[2] Y. Arava, Y. Wang, J. D. Storey, C. L. Liu, P. O. Brown, and D. Herschlag, "Genome-wide analysis of mRNA translation profiles in Saccharomyces cerevisiae," *Proceedings of the National Academy of Sciences*, vol. 100, no. 7, pp. 3889–3894, 2003.

[3] R. A. Blythe and M. R. Evans, "Nonequilibrium steady states of matrix-product form: a solver's guide," *J. Phys. A: Math. Gen.*, vol. 40, no. 46, pp. R333–R441, 2007.

[4] M. Bretscher, "Direct translation of a circular messenger DNA," *Nature*, vol. 220, no. 5172, pp. 1088–91, 1968.

[5] M. Bretscher, "Direct translation of bacteriophage fd DNA in the absence of neomycin B," *J. Mol. Biol.*, vol. 42, no. 3, pp. 595–8, 1969.

[6] C. E. Burd, W. R. Jeck, Y. Liu, H. K. Sanoff, Z. Wang, and N. E. Sharpless, "Expression of linear and novel circular forms of an INK4/ARF-associated non-coding RNA correlates with atherosclerosis risk," *PLoS Genet.*, vol. 6, p. e1001233, 2010.

[7] A. Capel, B. Swain, S. Nicolis, A. Hacker, M. Walter, P. Koopman, P. Goodfellow, and R. Lovell-Badge, "Circular transcripts of the testis-determining gene Sry in adult mouse testis," *Cell*, vol. 73, pp. 1019–1030, 1993.

[8] L. Cartegni, S. Chew, and A. Krainer, "Listening to silence and understanding nonsense: exonic mutations that affect splicing," *Nat. Rev. Genet.*, vol. 3, pp. 285–98, 2002.

[9] D. Chu, N. Zabet, and T. von der Haar, "A novel and versatile computational tool to model translation," *Bioinformatics*, vol. 28, no. 2, pp. 292–293, 2012.

[10] C. Cocquerelle, B. Mascrez, D. Hetuin, and B. Bailleul, "Mis-splicing yields circular RNA molecules," *FASEB J.*, vol. 7, pp. 155–160, 1993.

[11] A. Dana and T. Tuller, "Efficient manipulations of synonymous mutations for controlling translation rate–an analytical approach," *J. Comput. Biol.*, vol. 19, pp. 200–231, 2012.

[12] M. Danan, S. Schwartz, S. Edelheit, and R. Sorek, "Transcriptome-wide discovery of circular RNAs in Archaea," *Nucleic Acids Res.*, vol. 40, no. 7, pp. 3131–42, 2012.

[13] C. Deneke, R. Lipowsky, and A. Valleriani, "Effect of ribosome shielding on mRNA stability," *Phys. Biol.*, vol. 10, no. 4, p. 046008, 2013.

[14] D. A. Drummond and C. O. Wilke, "Mistranslation-induced protein misfolding as a dominant constraint on coding-sequence evolution," *Cell*, vol. 134, pp. 341–352, 2008.

[15] S. Edri and T. Tuller, "Quantifying the effect of ribosomal density on mRNA stability," *PLoS One*, vol. 9, p. e102308, 2014.

[16] R. Heinrich and T. Rapoport, "Mathematical modelling of translation of mRNA in eucaryotes; steady state, time-dependent processes and application to reticulocytes," *J. Theoretical Biology*, vol. 86, pp. 279–313, 1980.

[17] L. Hensgens, A. Arnberg, E. Roosendaal, G. van der Horst, R. van der Veen, G. van Ommen, and L. Grivell, "Variation, transcription and circular RNAs of the mitochondrial gene for subunit I of cytochrome c oxidase," *J. Mol. Biol.*, vol. 164, pp. 35–58, 1983.

[18] C. Kimchi-Sarfaty, T. Schiller, N. Hamasaki-Katagiri, M. Khan, C. Yanover, and Z. Sauna, "Building better drugs: developing and regulating engineered therapeutic proteins," *Trends Pharmacol. Sci.*, vol. 34, no. 10, pp. 534–548, 2013.

[19] C. Kurland, "Translational accuracy and the fitness of bacteria," *Annu Rev Genet.*, vol. 26, pp. 29–50, 1992.

[20] G. Li, D. Burkhardt, C. Gross, and J. Weissman, "Quantifying absolute protein synthesis rates reveals principles underlying allocation of cellular resources," *Cell*, vol. 157, no. 3, pp. 624–35, 2014.

[21] J. Lodge, P. Lund, and S. Minchin, *Gene Cloning: Principles and Applications*. Taylor and Francis, 2006.

[22] L. Lorentzen and H. Waadeland, *Continued Fractions: Convergence Theory*, 2nd ed. Paris: Atlantis Press, 2008, vol. 1.

[23] C. T. MacDonald, J. H. Gibbs, and A. C. Pipkin, "Kinetics of biopolymerization on nucleic acid templates," *Biopolymers*, vol. 6, pp. 1–25, 1968.

[24] M. Margaliot, E. D. Sontag, and T. Tuller, "Entrainment to periodic initiation and transition rates in a computational model for gene translation," *PLoS ONE*, vol. 9, no. 5, p. e96039, 2014.

[25] M. Margaliot and T. Tuller, "Stability analysis of the ribosome flow model," *IEEE/ACM Trans. Computational Biology and Bioinformatics*, vol. 9, pp. 1545–1552, 2012.

[26] M. Margaliot and T. Tuller, "Ribosome flow model with positive feedback," *J. Royal Society Interface*, vol. 10, p. 20130267, 2013.

[27] E. Marshall, I. Stansfield, and M. Romano, "Ribosome recycling induces optimal translation rate at low ribosomal availability," *J. Royal Society Interface.*, vol. 11, no. 98, p. 20140589, 2014.

[28] T. Morisaki, K. Lyon, K. F. DeLuca, J. G. DeLuca, B. P. English, Z. Zhang, L. D. Lavis, J. B. Grimm, S. Viswanathan, L. L. Looger, T. Lionnet, and T. J. Stasevich, "Real-time quantification of single RNA translation dynamics in living cells," *Science*, vol. 352, no. 6292, pp. 1425–9, 2016.

[29] S. Pechmann and J. Frydman, "Evolutionary conservation of codon optimality reveals hidden signatures of cotranslational folding," *Nat Struct Mol Biol.*, vol. 20, no. 2, pp. 237–43, 2013.

[30] F. Picard, P. Loubiere, and M. Girbal, L. Cocaign-Bousquet, "The significance of translation regulation in the stress response," *BMC Genomics*, vol. 14, p. 588, 2013.

[31] M. Piques, W. Schulze, M. Hohne, B. Usadel, Y. Gibon, J. Rohwer, and S. M., "Ribosome and transcript copy numbers, polysome occupancy and enzyme dynamics in Arabidopsis," *Mol Syst Biol.*, vol. 5, p. 314, 2009.

[32] G. Poker, Y. Zarai, M. Margaliot, and T. Tuller, "Maximizing protein translation rate in the nonhomogeneous ribosome flow model: A convex optimization approach," *J. Royal Society Interface*, vol. 11, no. 100, p. 20140713, 2014.

[33] G. Poker, M. Margaliot, and T. Tuller, "Sensitivity of mRNA translation," *Sci. Rep.*, vol. 5, p. 12795, 2015.

[34] S. Proshkin, A. Rahmouni, A. Mironov, and E. Nudler, "Cooperation between translating ribosomes and RNA polymerase in transcription elongation," *Science*, vol. 328, no. 5977, pp. 504–508, 2010.

[35] R. Pugatch, "Greedy scheduling of cellular self-replication leads to optimal doubling times with a log-Frechet distribution," *Proceedings of the National Academy of Sciences*, vol. 112, no. 8, pp. 2611–2616, 2015.

[36] J. Racle, F. Picard, L. Girbal, M. Cocaign-Bousquet, and V. Hatzimanikatis, "A genome-scale integration and analysis of Lactococcus lactis translation data," *PLOS Computational Biology*, vol. 9, no. 10, p. e1003240, 2013.

[37] J. Racle, J. Overney, and V. Hatzimanikatis, "A computational framework for the design of optimal protein synthesis," *Biotechnology and Bioengineering*, vol. 109, no. 8, pp. 2127–2133, 2012.

[38] A. Raveh, Y. Zarai, M. Margaliot, and T. Tuller, "Ribosome flow model on a ring," *IEEE/ACM Trans. Computational Biology and Bioinformatics*, vol. 12, no. 6, pp. 1429–1439, 2015.

[39] A. Raveh, M. Margaliot, E. D. Sontag, and T. Tuller, "A model for competition for ribosomes in the cell," *J. Royal Society Interface*, vol. 13, no. 116, 2016.

[40] S. Reuveni, I. Meilijson, M. Kupiec, E. Ruppin, and T. Tuller, "Genome-scale analysis of translation elongation with a ribosome flow model," *PLOS Computational Biology*, vol. 7, p. e1002127, 2011.

[41] A. Schadschneider, D. Chowdhury, and K. Nishinari, *Stochastic Transport in Complex Systems: From Molecules to Vehicles*. Elsevier, 2011.

[42] P. Shah, Y. Ding, M. Niemczyk, G. Kudla, and J. Plotkin, "Rate-limiting steps in yeast protein translation," *Cell*, vol. 153, no. 7, pp. 1589–601, 2013.

[43] L. B. Shaw, R. K. P. Zia, and K. H. Lee, "Totally asymmetric exclusion process with extended objects: a model for protein synthesis," *Phys. Rev. E*, vol. 68, p. 021910, 2003.

[44] H. L. Smith, *Monotone Dynamical Systems: An Introduction to the Theory of Competitive and Cooperative Systems*, ser. Mathematical Surveys and Monographs. Providence, RI: Amer. Math. Soc., 1995, vol. 41.

[45] E. D. Sontag, "Some new directions in control theory inspired by systems biology," *IEE Proceedings-Systems Biology*, vol. 1, no. 1, pp. 9–18, 2004.

[46] E. D. Sontag, "Molecular systems biology and control," *Euro. J. Control*, vol. 11, no. 4, pp. 396–435, 2005.

[47] A. Stergachis, E. Haugen, A. Shafer, W. Fu, B. Vernot, A. Reynolds, A. Raubitschek, S. Ziegler, E. LeProust, J. Akey, and J. Stamatoyannopoulos, "Exonic transcription factor binding directs codon choice and affects protein evolution," *Science*, vol. 342, pp. 1367–72, 2013.

[48] R. Subramaniam, A, B. Zid, and E. O'Shea, "An integrated approach reveals regulatory controls on bacterial translation elongation," *Cell*, vol. 159, no. 5, pp. 1200–11, 2014.

[49] T. Tuller, A. Carmi, K. Vestsigian, S. Navon, Y. Dorfan, J. Zaborske, T. Pan, O. Dahan, I. Furman, and Y. Pilpel, "An evolutionarily conserved mechanism for controlling the efficiency of protein translation," *Cell*, vol. 141, no. 2, pp. 344–54, 2010.

[50] T. Tuller, M. Kupiec, and E. Ruppin, "Determinants of protein abundance and translation efficiency in s. cerevisiae." *PLOS Computational Biology*, vol. 3, pp. 2510–2519, 2007.

[51] T. Tuller, I. Veksler, N. Gazit, M. Kupiec, E. Ruppin, and M. Ziv, "Composite effects of gene determinants on the translation speed and density of ribosomes," *Genome Biol.*, vol. 12, no. 11, p. R110, 2011.

[52] T. Tuller and H. Zur, "Multiple roles of the coding sequence 5' end in gene expression regulation," *Nucleic Acids Res.*, vol. 43, no. 1, pp. 13–28, 2015.

[53] C. Wang, B. Han, R. Zhou, and X. Zhuang, "Real-time imaging of translation on single mRNA transcripts in live cells," *Cell*, vol. 165, no. 4, pp. 990–1001, 2016.

[54] S. Wells, P. Hillner, R. Vale, and A. Sachs, "Circularization of mRNA by eukaryotic translation initiation factors," *Mol. Cell*, vol. 2, no. 1, pp. 135–40, 1998.

[55] B. Wu, C. Eliscovich, Y. Yoon, and R. Singer, "Translation dynamics of single mRNAs in live cells and neurons," *Science*, vol. 352, no. 6292, pp. 1430–5, 2016.

[56] X. Yan, T. A. Hoek, R. D. Vale, and M. E. Tanenbaum, "Dynamics of translation of single mRNA molecules in vivo," *Cell*, vol. 165, no. 4, pp. 976–89, 2016.

[57] A. Yonath, "Ribosomes: Ribozymes that survived evolution pressures but is paralyzed by tiny antibiotics," in *Macromolecular Crystallography: Deciphering the Structure, Function and Dynamics of Biological Molecules*, A. M. Carrondo and P. Spadon, Eds. Dordrecht: Springer Netherlands, 2012, pp. 195–208.

[58] Z. Zafrir and T. Tuller, "Nucleotide sequence composition adjacent to intronic splice sites improves splicing efficiency via its effect on pre-mrna local folding in fungi," *RNA*, vol. 21, no. 10, pp. 1704–18, 2015.

[59] Y. Zarai and M. Margaliot, "On minimizing the maximal characteristic frequency of a linear chain," *IEEE Trans. Automat. Control*, 2016, to appear.

[60] Y. Zarai, M. Margaliot, E. D. Sontag, and T. Tuller, "Controlling mRNA translation," 2016, submitted. [Online]. Available: http://arxiv.org/abs/1602.02308

[61] Y. Zarai, M. Margaliot, and T. Tuller, "Explicit expression for the steady-state translation rate in the infinite-dimensional homogeneous ribosome flow model," *IEEE/ACM Trans. Computational Biology and Bioinformatics*, vol. 10, pp. 1322–1328, 2013.

[62] Y. Zarai, O. Mendel, and M. Margaliot, “Analyzing linear communication networks using the ribosome flow model,” in *Proc. 15th IEEE International Conf. on Computer and Information Technology*, Liverpool, UK, 2015.

[63] G. Zhang, M. Hubalewska, and Z. Ignatova, “Transient ribosomal attenuation coordinates protein synthesis and co-translational folding,” *Nat Struct Mol Biol.*, vol. 16, no. 3, pp. 274–280, 2009.

[64] S. Zhang, E. Goldman, and G. Zubay, “Clustering of low usage codons and ribosome movement,” *J. Theoretical Biology*, vol. 170, pp. 339–354, 1994.

[65] R. K. P. Zia, J. Dong, and B. Schmittmann, “Modeling translation in protein synthesis with TASEP: A tutorial and recent developments,” *J. Statistical Physics*, vol. 144, pp. 405–428, 2011.

[66] H. Zouridis and V. Hatzimanikatis, “A model for protein translation: Polysome self-organization leads to maximum protein synthesis rates,” *Biophysical J.*, vol. 92, no. 3, pp. 717–730, 2007.